

Nucleation in Finite Topological Systems During Continuous Metastable Quantum Phase Transitions

Oleksandr Fialko,¹ Marie-Coralie Delattre,¹ Joachim Brand,¹ and Andrey R. Kolovsky^{2,3}

¹Centre for Theoretical Chemistry and Physics and New Zealand Institute for Advanced Study, Massey University, Private Bag 102904 NSMC, Auckland 0745, New Zealand

²Kirensky Institute of Physics, 660036 Krasnoyarsk, Russia

³Siberian Federal University, 660041 Krasnoyarsk, Russia

(Received 22 February 2012; published 20 June 2012)

Finite topological quantum systems can undergo continuous metastable quantum phase transitions to change their topological nature. Here we show how to nucleate the transition between ring currents and dark soliton states in a toroidally trapped Bose-Einstein condensate. An adiabatic passage to wind and unwind its phase is achieved by explicit global breaking of the rotational symmetry. This could be realized with current experimental technology.

DOI: [10.1103/PhysRevLett.108.250402](https://doi.org/10.1103/PhysRevLett.108.250402)

PACS numbers: 05.30.Rt, 03.75.Nt, 67.10.Ba

Phase transitions have long been considered equilibrium phenomena of infinite systems that can involve interesting nonequilibrium nucleation dynamics, e.g., the formation of topological defects [1]. In recent years, quantum phase transitions have also been identified in excited states of nuclei as well as ultracold quantum gases [2–5] by the nonanalytic change in spectral properties, or their finite-system precursors, as a system parameter is changed. Such phase transitions are not manifested in equilibrium but they have dynamical consequences [3,4]. So far, little is known about the nucleation process.

Nucleation of equilibrium quantum phase transitions often relies on external symmetry breaking, which can occur *locally*. An example is the Ising model [6], where a tiny external magnetic field is sufficient for breaking the rotational symmetry of the spins and allowing the system to equilibrate. Similar mechanisms were discussed in the context of vortex nucleation in Bose gases [7–9]. Here we theoretically investigate the quantum phase transition between metastable states of a Bose gas in a rotating toroidal trap identified in Ref. [5]. The transition occurs between topological *vortex states* and nontopological *soliton states*. Vortex states of N atoms correspond to ring currents and carry integer angular momentum per particle $L/(N\hbar) = J$. As the rotation frequency of the trap Ω is changed, the ground state jumps between vortex states [10] and thus the integer J is a topological charge. The soliton states carry noninteger $L/(N\hbar)$. In mean-field theory they are approximated by dark solitons [11], which carry a localized density notch and thus break rotational symmetry in addition to changing the topological nature of the system, although no symmetry breaking is required for the phase transition in the quantum description of the finite system.

In this Letter, we show how to nucleate the phase transition by means of a *global* symmetry-breaking potential, which creates an adiabatic passage through metastable states. Although symmetry can be restored for a finite

system, the passage naturally leads to the emergence of symmetry-broken soliton solutions for large particle number N . In order to maintain metastability, we further find that local symmetry breaking needs to be avoided as it would lead to the unwanted thermalization of the excited states [12]. This is in stark contrast to equilibrium phase transitions, where thermalization is desirable. The explicit global symmetry breaking is achieved by tilting the trap axis by some angle θ and rotating it with the frequency Ω . The frequency Ω is decreased from a maximum value Ω_{initial} to a minimum value Ω_{final} within a finite time interval, after which the tilt is decreased. Under certain conditions angular momentum is established in the Bose gas up to a dark soliton state or a vortex state as seen in Figs. 1 and 2, respectively. The protocol is counterintuitive as we decrease the rotation frequency of the system to increase its angular momentum. It is reminiscent of the stimulated Raman adiabatic passage used in quantum optics to populate a metastable state through an intermediate level by a counterintuitive pulse sequence [13].

Interacting bosonic atoms of mass m confined to a rotating toroidal trap are described by the Hamiltonian

$$\hat{H} = \int dx \hat{\Psi}^\dagger \left[-\frac{\hbar^2}{2m} \frac{\partial^2}{\partial x^2} + \frac{U}{2} \hat{\Psi}^\dagger \hat{\Psi} + \epsilon \cos\left(\frac{x}{R} - \Omega t\right) \right] \hat{\Psi}, \quad (1)$$

where $\hat{\Psi} \equiv \hat{\Psi}(x)$ is the atomic field operator, U the bare interaction constant that is assumed repulsive ($U > 0$), and $\epsilon = mgR \sin(\theta)$ the strength of the symmetry-breaking potential (where mg is the gravitational force). The toroidal trap is approximated by a one-dimensional ring of radius R .

Let us first discuss the outlined problem in the mean-field approximation. Using a rotating coordinate frame with frequency Ω and introducing the scaled variables

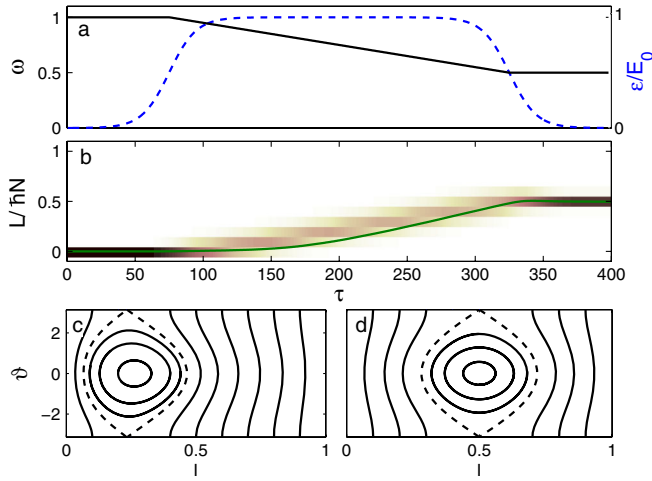


FIG. 1 (color online). Adiabatic passage from the ground to the dark soliton state. (a) Protocol for variations of the perturbation parameter ϵ (dashed line) and the precession frequency ω (full line) for $\gamma = 0.8E_0$. (b) Angular momentum per particle in the mean-field approximation [Eq. (2)] over time (full line) and probability density of the quantum two-mode simulation with the Hamiltonian [Eq. (9)] on the same axes. White and black correspond to zero and maximum probability density, respectively. Phase portraits of Eq. (3) are presented for $\omega = 0.7$ (c) and $\omega = 0.5$ (d).

$\phi = x/R$, $\tau = tE_0/\hbar$, $\omega = \hbar\Omega/(2E_0)$, the Gross-Pitaevskii (GP) equation reads [11]

$$i\frac{\partial\chi}{\partial\tau} = \left[-(\partial_\phi - i\omega)^2 + 2\pi\frac{\gamma}{E_0}|\chi|^2 + \frac{\epsilon}{E_0}\cos(\phi) \right]\chi, \quad (2)$$

where $\gamma = U(N-1)/(2\pi R)$ and $E_0 = \hbar^2/(2mR^2)$ gives the relevant energy scale. The classical field χ is normalized as $\int_0^{2\pi} |\chi|^2 d\phi = 1$ and it is periodic on ϕ , $\chi(0) = \chi(2\pi)$. We apply Broyden's method [14] to solve Eq. (2) numerically for the stationary solutions $\chi(\tau, \phi) = \chi(\phi)e^{-i\mu\tau}$, where μE_0 is the chemical potential. For $\epsilon = 0$ we present in Fig. 3(a) three solutions corresponding to two vortex states $\chi(\phi) = e^{iJ\phi}/\sqrt{2\pi}$ with $J = 0$ and $J = 1$, which are connected by a soliton branch. Finite ϵ opens a gap in the soliton branch, see Fig. 3(b). The lower branch corresponds to a soliton sitting on the crest, while the upper branch connects to a soliton located in the trough of the external potential. In the following we will show that the lower branch is dynamically unstable, while the upper branch is stable. Thus an adiabatic passage through the upper branch is possible. Numerical simulations of the system dynamics on the basis of Eq. (2) confirm this expectation. The solid lines in Figs. 1(b) and 2(b) show the momentum per atom as a function of time for the adiabatic protocols shown in the top panels. The final soliton and vortex states are shown in Figs. 2(c) and 2(d), respectively.

Mean-field theory thus presents the following picture: the bifurcation points between the soliton and vortex

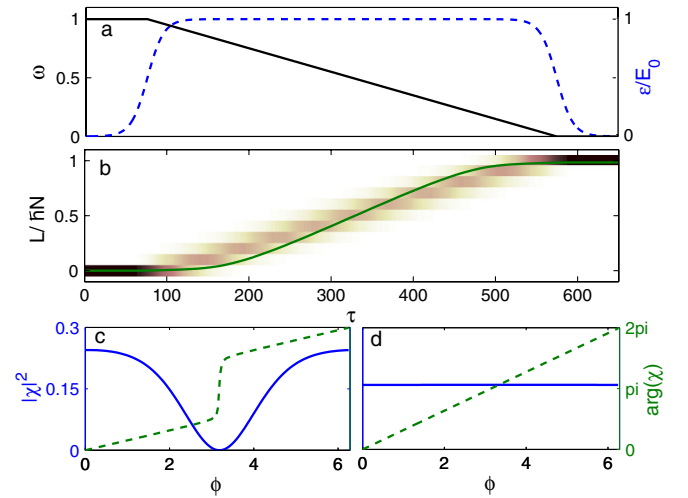


FIG. 2 (color online). Adiabatic passage from the ground state to the $J = 1$ vortex state. (a) Protocol for variations of the perturbation parameter ϵ (dashed line) and the precession frequency ω (full line) for $\gamma = 0.8E_0$. (b) Angular momentum per particle in the mean-field approximation (full line) and probability density of the corresponding quantum simulation as in Fig. 1. The dark soliton state (c) and the vortex state (d) represent the final states of the corresponding mean-field simulations. Full lines represent density, dashed lines represent phases.

branches seen in Fig. 3(a) mark the transition between rotationally symmetric, and symmetry-broken [Fig. 2(c)] phases. With finite ϵ , the symmetry is formally broken everywhere and the bifurcation makes way to a swallowtail structure [15] in Fig. 3(b). In contrast to the dynamics of continuous phase transitions in infinite systems where

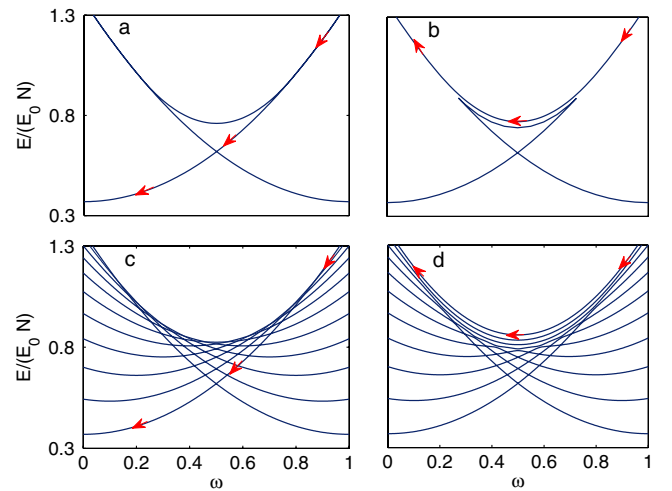


FIG. 3 (color online). The energy of the GP equation (upper row) and the energy spectrum of the Hamiltonian [Eq. (9)] in the two-mode approximation (lower row). Parameters are $\gamma = 0.8E_0$, and $\epsilon = 0$ (left column) and $\epsilon = 0.04E_0$ (right column). The arrows show the passage under adiabatic change of the frequency ω . Three distinct solutions exist in panel (a) between the bifurcation points $\omega_- \approx 0.13$ and $\omega_+ \approx 0.87$.

adiabaticity is always violated [1], an adiabatic passage is established (arrows in Fig. 3) to change the symmetry properties of the initial state. Due to the global nature of the symmetry-broken state with a single soliton in the whole ring there is no formation of domain structures with locally broken symmetry in further contrast to Ref. [1].

We proceed with discussing and quantifying the necessary conditions for an adiabatic passage. Useful insight into the physics of the considered process is obtained within a two-mode approximation, which is justified for small $\gamma \ll E_0$. Neglecting all coefficients in the Fourier expansion except $k = 0, 1$ of the function χ , $\chi(\tau, \phi) = \sum_k b_k(\tau) \exp(ik\phi)$, the system dynamics is described by the effective Hamiltonian

$$H_{\text{cl}} = E_0(1 - 2\omega)I + \gamma I(1 - I) + \epsilon\sqrt{I(1 - I)}\cos\vartheta, \quad (3)$$

where $I = |b_1|^2$ and ϑ is the relative phase for the amplitudes b_0 and b_1 . The phase portrait of Eq. (3) contains a stability island around the elliptic point $(I, \vartheta) = (I^*, 0)$ [cf. Figs. 1(c) and 1(d)], where $I^* \approx 1/2 + (1/2 - \omega)E_0/\gamma$ depends linearly on ω and reaches values of zero and unity for

$$\omega_{\pm} = \frac{1}{2} \pm \frac{\gamma}{2E_0}, \quad (4)$$

respectively. We note that in the lab frame this stability island corresponds to a nonlinear resonance. Thus the adiabatic passage has a simple physical interpretation: by ramping ϵ to a finite value we capture the system into the nonlinear resonance, transport it to any desired value of I by adiabatically changing the frequency ω from $\omega_{\text{initial}} \geq \omega_+$ to ω_{final} , and release the system by ramping ϵ back to zero. The necessary condition for the time scale of this process is $\Delta t \gg \Omega_s^{-1}$, where $\Omega_s \approx \sqrt{\gamma\epsilon}/\hbar$ is the frequency of small oscillations near the elliptic point of the stability island (the approximate sign is replaced by an equal sign for $\omega = 1/2$).

For stronger nonlinearity, $\gamma > E_0$, when the two-mode approximation is not justified, the adiabaticity conditions and stability can be studied using the Bogoliubov approach, which linearizes the time dependent GP equation [Eq. (2)] [11]. This leads to the eigenvalue problem

$$\begin{aligned} \lambda_i u_i &= (\hat{H}_{\text{GP}} - \mu + 2\pi\gamma/E_0|\chi|^2)u_i + 2\pi\gamma/E_0\chi^2 v_i, \\ -\lambda_i v_i &= (\hat{H}_{\text{GP}} - \mu + 2\pi\gamma/E_0|\chi|^2)v_i + 2\pi\gamma/E_0\chi^{*2} u_i. \end{aligned} \quad (5)$$

Here, $\chi = \chi_{\omega}(\phi)$ is the stationary solution for the upper soliton branch in Fig. 3(b) and \hat{H}_{GP} is given in the square brackets in Eq. (2). For the lower branch we find a single imaginary eigenvalue λ , which indicates that the solutions on this branch are dynamically unstable [11]. The Bogoliubov analysis for the upper branch indicates that it is dynamically stable and that there is a gap to the lowest

lying elementary excitation. The corresponding frequency $\Omega_s = \lambda E_0/\hbar$ has the asymptotic behavior

$$\Omega_s = \begin{cases} \sqrt{\gamma\epsilon}/\hbar, & \gamma \ll E_0 \\ \sqrt{E_0\epsilon}/\hbar, & \gamma \gg E_0 \end{cases}. \quad (6)$$

For small nonlinearities where $\gamma \ll E_0$ this result agrees with the previous two-mode analysis.

The large γ result can be understood by noting that the soliton is a localized object. In this case Ω_s is interpreted as the frequency of small oscillations of the soliton around a stationary point. Indeed, it can be shown that the small oscillations of the soliton around the stationary points are described by the equation [16]

$$m\left(\frac{\partial\phi_s}{\partial t}\right)^2 \pm \frac{\epsilon}{2R^2}\phi_s^2 \approx \text{const}, \quad (7)$$

which is valid for $\Omega \approx E_0/\hbar$. The \pm sign corresponds to a soliton sitting at the trough or the crest of the potential, respectively. While the minus sign describes an unstable situation [lower soliton branch in Fig. 3(b)], the plus sign describes harmonic oscillations of a particle with mass $2m$. The soliton located in the trough is thus dynamically stable, with the frequency of small oscillations $\Omega_s = \sqrt{\epsilon/(2mR^2)} = \sqrt{E_0\epsilon}/\hbar$.

In practice, the adiabaticity condition $\Delta t \gg \Omega_s^{-1}$ discussed above should be made even stronger by requiring that accelerated rotation should displace the soliton by less than the the soliton core size, which is of the order of the healing length $\xi = \sqrt{\hbar^2/2m\gamma}$. This yields the condition

$$\frac{\partial\Omega}{\partial t} \ll \frac{\xi}{R} \frac{E_0\epsilon}{\hbar^2}. \quad (8)$$

The numerical simulation of the system dynamics confirms the estimate of Eq. (8). For the parameters of Fig. 1 the right hand side of Eq. (8) is $\approx 0.04(E_0/\hbar)^2$. It is seen in Figs. 1(b) and 2(b) that for a ten times smaller rate $\dot{\Omega} = 0.004(E_0/\hbar)^2$ the dark soliton and the vortex states [green (solid) lines] are reached.

The mean-field analysis presented so far can be substantiated by a quantum analysis. Using scaled variables and a rotating coordinate frame, and expanding the field operators in the angular-momentum basis, the Hamiltonian of the system takes the form of the Lieb-Liniger Hamiltonian [17] with an external symmetry-breaking potential under periodic boundary conditions

$$\begin{aligned} \hat{H} &= E_0 \sum_k (k - \omega)^2 \hat{b}_k^\dagger \hat{b}_k + \frac{\epsilon}{2} \sum_k (\hat{b}_{k+1}^\dagger \hat{b}_k + \text{H.c.}) \\ &+ \frac{U}{4\pi R} \sum_{k_1, k_2, k_3, k_4} \hat{b}_{k_1}^\dagger \hat{b}_{k_2}^\dagger \hat{b}_{k_3} \hat{b}_{-k_3 - k_2 - k_1}. \end{aligned} \quad (9)$$

We are interested in the time evolution with initial condition given by the nonrotating ground state (vortex state with $J = 0$). The soliton states have definite angular

momentum for $\epsilon = 0$ and, within the validity of the two-mode approximation, are given by

$$|\psi_l\rangle = (\hat{b}_0^\dagger)^{N-l}(\hat{b}_1^\dagger)^l|\text{vac}\rangle. \quad (10)$$

Truncating the Fock basis to the states [Eq. (10)], the Hamiltonian [Eq. (9)] is a tridiagonal $(N+1) \times (N+1)$ matrix. Figure 3(c) shows the spectrum of this matrix for $N = 10$, $\gamma = 0.8E_0$, $\epsilon = 0$, and $0 \leq \omega \leq 1$. Note that for $U = 0$ all levels would cross at one point at $\omega = 1/2$. Finite interactions remove this degeneracy, leading to the appearance of a caustic in the level crossing pattern. The spectrum of the system for a finite $\epsilon = 0.04E_0$ is shown in Fig. 3(d) [18]. Now all level crossings are substituted by avoided crossings. The Hamiltonian in the two-mode model can be recast to take the form of a quantized version of the effective Hamiltonian [Eq. (3)], where the action variable I is now associated with the operator $\hat{I} = -i(1/N)\partial/\partial\vartheta$ and $1/N$ plays the role of the Planck constant. In particular, we find that the transition frequency between the caustic levels is given by Ω_s of Eq. (6).

Within the quantum model we can find a condition for the frequency ω_{initial} from the crossing point of the two energy levels that are lowest for $\omega = 0$ in Fig. 3(c). In the two-mode approximation, we obtain ω_+ of Eq. (4), the same result as from the mean-field analysis. A more thorough comparison of the upper and lower rows in Fig. 3 indicates that energies of the soliton states calculated within the mean-field approximation are shifted in the negative direction compared to the quantum calculation. This is a manifestation of the occupation of additional angular momentum modes outside the two-mode model. In order to extend the result for ω_+ beyond the two-mode approximation, we consider the rotation frequency $\omega_l = \sqrt{l^2 + 2\gamma/E_0}/2$ where the Bogoliubov phonon with angular momentum $l\hbar > 0$ acquires zero energy. The expression for $\omega_+ \equiv \omega_l$ thereby generalizes Eq. (4) to larger values of γ . Generally, it looks possible to excite the vortex state with topological charge J with the condition $\omega_J < \omega_{\text{initial}} < \omega_{J+1}$ (see Supplemental Material [19]) through metastable states with J dark solitons [5].

It is interesting to simulate the dynamics of the quantum system [Eq. (9)] for the same protocols as were used in the mean-field simulations. Due to exponential proliferation of the Hilbert space with N , this can be done only for a small number of atoms, $N \sim 10$. The density plots of Figs. 1(b) and 2(b) show the dynamics of the system [Eq. (9)] in the two-mode approximation for $N = 10$ and $\gamma = 0.8E_0$. (We have checked that for these values of the interaction constant and number of particles the result remains unchanged if we use a four-mode approximation.) The gray scale encodes populations of the Fock states [Eq. (10)]. It is seen in Figs. 1 and 2 that our protocols almost entirely populate the target excited state $|\psi_{N/2}\rangle$ [Fig. 1(b)] and $|\psi_N\rangle$ [Fig. 2(b)], respectively, with the probabilities 0.93 and 1.

The quantum model [Eq. (9)] reveals why global symmetry breaking is effective for nucleating the metastable phase transition: the long wavelength perturbing potential proportional to ϵ couples neighboring soliton states [Eq. (10)] effectively and thus creates the avoided crossings that provide the adiabatic passage. A short wavelength, *local* symmetry-breaking perturbation, in contrast, would tentatively couple to excited states with larger angular momentum difference, generate drag, and thus compromise the adiabatic passage. For a large system ($R \gg \xi$) this is expected from both quantum [10] and mean-field [20] consideration of a localized impurity moving at supersonic velocity $\Omega R > \Omega_1 R = c + \mathcal{O}(R^{-1})$, where $c = \sqrt{\gamma/m}$ is the speed of sound.

There is still a crucial difference between the quantum and mean-field models: while the soliton states of the GP approximation break the rotational symmetry, the corresponding quantum states [Eq. (10)] do not. Instead, they correspond to fragmented condensates, where both the occupation of the $k = 0$ and the $k = 1$ mode can become large. Whether we obtain a fragmented condensate with preserved rotational symmetry or a condensate with broken symmetry, depends on the rate for changing the parameter ϵ at the very end of the passage. A simple calculation reveals that the adiabatic condition is fulfilled if the rate satisfies $d\epsilon/dt \ll \gamma^2/(2\hbar N)$ [21]. For large N it becomes more difficult to restore symmetry, since the time scales required for restoring the symmetry become large. When ϵ is changed back to zero in finite time, the system ‘sits’ on the caustic where the density of states tends to infinity if $N \rightarrow \infty$. That a large particle number brings a qualitative change is familiar from the general principle of symmetry breaking in condensed matter [22]. In contrast to conventional phase transitions, however, where symmetry breaking occurs spontaneously, the metastable quantum phase transition discussed in this Letter requires an explicit breaking of its symmetry.

So far we have mostly considered the case of moderate nonlinearity, where the two-mode approximation is justified. In typical experiments with Bose-Einstein condensates, larger nonlinearities beyond the validity of the two-mode approximation are relevant. We have verified within the mean-field theory that adiabatic passage for stronger nonlinearities is possible as well (see Supplemental Material [19]). We estimate the time scale for the adiabatic passage to a dark soliton state using Eq. (8) and setting $\epsilon \sim \gamma$ as $\Delta t \gg mR^2/\hbar$. In the recent experiment with ^{23}Na [23], $R \sim 20 \mu\text{m}$. This gives $\Delta t \gg 1\text{s}$. For lighter atoms, e.g., ^7Li , and smaller radius, e.g., $R \sim 10 \mu\text{m}$, one can achieve the condition $\Delta t \gg 0.1\text{s}$ and $\theta \approx 0.5^\circ$. Therefore, time scales of the order of 1s will provide an adiabatic passage.

In conclusion, we have proposed an experimental scheme to nucleate a metastable quantum phase transition in an ultracold Bose gas by an adiabatic passage. We have shown that this is achieved by an explicit breaking of the

global rotational symmetry. The procedure generalizes nucleation procedures, which change the ground state symmetries in the course of ordinary continuous phase transitions.

We acknowledge stimulating discussions with Jean-Sebasti en Caux and Lincoln Carr. A.K. thanks Massey University for hospitality. O.F., M.C.D., and J.B. were supported by the Marsden Fund (Contract No. MAU0910) administered by the Royal Society of New Zealand.

-
- [1] W.H. Zurek, *Nature (London)* **317**, 505 (1985); R.D. Averitt, *Nature Phys.* **6**, 639 (2010); R. Yusupov, T. Mertelj, V.V. Kabanov, S. Brazovskii, P. Kusar, J.-H. Chu, I.R. Fisher, and D. Mihailovic, *ibid.* **6**, 681 (2010); A. Das, J. Sabbatini, and W.H. Zurek, *Sci. Rep.* **2**, 352 (2012).
- [2] L.D. Carr, *Understanding Quantum Phase Transitions* (Taylor and Francis, London, 2010).
- [3] M. A. Caprio, P. Cejnar, and F. Iachello, *Ann. Phys. (N.Y.)* **323**, 1106 (2008).
- [4] V.S. Shchesnovich and V.V. Konotop, *Phys. Rev. Lett.* **102**, 055702 (2009).
- [5] R. Kanamoto, L.D. Carr, and M. Ueda, *Phys. Rev. Lett.* **100**, 060401 (2008); R. Kanamoto, L.D. Carr, and M. Ueda, *Phys. Rev. A* **79**, 063616 (2009).
- [6] S. Sachdev and B. Keimer, *Phys. Today* **64**, No. 2, 29 (2011).
- [7] D. Dagnino, N. Barberan, M. Lewenstein, and J. Dalibard, *Nature Phys.* **5**, 431 (2009); A. Nunnenkamp, A. Rey, and K. Burnett, *Proc. R. Soc. A* **466**, 1247 (2010).
- [8] M. Hiller, T. Kottos, and D. Cohen, *Europhys. Lett.* **82**, 40006 (2008); M. Hiller, T. Kottos, and D. Cohen, *Phys. Rev. A* **78**, 013602 (2008).
- [9] D.W. Hallwood and J. Brand, *Phys. Rev. A* **84**, 043620 (2011).
- [10] A. Yu. Cherny, J.-S. Caux, and J. Brand, *Phys. Rev. A* **80**, 043604 (2009).
- [11] L. Pitaevskii and S. Stringari, *Bose-Einstein Condensation* (Oxford University, New York, 2003).
- [12] M. Srednicki, *Phys. Rev. E* **50**, 888 (1994); M. Rigol, V. Dunjko, and M. Olshanii, *Nature (London)* **452**, 854 (2008).
- [13] N.V. Vitanov, M. Fleischhauer, B.W. Shore, and K. Bergmann, *Adv. At. Mol. Opt. Phys.* **46**, 55 (2001).
- [14] C.G. Broyden, *Math. Comput.* **19**, 577 (1965).
- [15] E.J. Mueller, *Phys. Rev. A* **66**, 063603 (2002).
- [16] V.V. Konotop and L. Pitaevskii, *Phys. Rev. Lett.* **93**, 240403 (2004).
- [17] E.H. Lieb and W. Liniger, *Phys. Rev.* **130**, 1605 (1963).
- [18] We note in passing that a similar level crossing pattern appears in the problem of the nonlinear Landau-Zener tunnelling. See D. Witthaut, E.M. Graefe, and H.J. Korsch, *Phys. Rev. A* **73**, 063609 (2006); B. Wu and J. Liu, *Phys. Rev. Lett.* **96**, 020405 (2006).
- [19] See Supplemental Material at <http://link.aps.org/supplemental/10.1103/PhysRevLett.108.250402> for corresponding simulations.
- [20] V. Hakim, *Phys. Rev. E* **55**, 2835 (1997); M. Haddad and V. Hakim, *Phys. Rev. Lett.* **87**, 218901 (2001).
- [21] L.I. Schiff, *Quantum Mechanics* (Mcgraw-Hill, New York, 1968).
- [22] P.W. Anderson, *Science* **177**, 393 (1972).
- [23] A. Ramanathan, K.C. Wright, S.R. Muniz, M. Zelan, W.T. Hill, C.J. Lobb, K. Helmerson, W.D. Phillips, and G.K. Campbell, *Phys. Rev. Lett.* **106**, 130401 (2011).